

ORIGINAL ARTICLE

Computed Tomography Findings in Xanthogranulomatous Pyelonephritis

Arumugam Rajesh, George Jakanani, Nick Mayer¹, Kevin Mulcahy

Departments of Clinical Radiology and ¹Pathology, University Hospitals of Leicester NHS Trust, Leicester General Hospital, Gwendolen Road, Leicester LE5 4PW, United Kingdom

Address for correspondence:

Dr. Arumugam Rajesh,
Department of Clinical Radiology,
University Hospitals of Leicester
NHS Trust, Leicester General
Hospital, Gwendolen Road,
Leicester LE5 4PW, United Kingdom.
E-mail: arajesh27@hotmail.com



Received : 16-06-2011

Accepted : 01-08-2011

Published : 27-08-2011

ABSTRACT

Background: Xanthogranulomatous pyelonephritis (XGN) is an uncommon condition characterized by chronic suppurative renal inflammation that leads to progressive parenchymal destruction. **Purpose:** To review the computed tomography (CT) findings of patients diagnosed with XGN. **Materials and Methods:** A retrospective review of CT findings in patients with histologically proven XGN was carried out. **Results:** Thirteen CT examinations of 11 patients were analyzed. Renal enlargement was demonstrable on the affected side in all patients. Nine patients (82%) had multiple dilated calyces and abnormal parenchyma. Six patients (55%) had a renal pelvis or upper ureteric calculus causing obstruction. Three patients (27%) had focal fat deposits identifiable within the inflamed renal parenchyma. Two patients had renal abscesses. Ten patients (91%) had extrarenal extension of the inflammatory changes. Three patients (27%) demonstrated extensive retroperitoneal inflammation. **Conclusion:** Unilateral renal enlargement and inflammation were the most consistent findings of XGN on CT. Perinephric inflammation and collections or abscess should also alert the radiologist to the possibility of this diagnosis.

Key words: Xanthogranulomatous pyelonephritis, computed tomography, perinephric inflammation

INTRODUCTION

Xanthogranulomatous pyelonephritis (XGN) is an uncommon condition characterized by chronic suppurative renal inflammation that leads to progressive parenchymal destruction.^[1] In the past, the preoperative diagnosis of XGN was notoriously difficult because of its nonspecific clinical

presentation and nonspecific radiographic appearances. The ability to diagnose XGN preoperatively has considerably improved with the use of ultrasound and computed tomography (CT). The aim of this study was to review and describe the CT findings in patients diagnosed with XGN from our institution in the past 5 years.

MATERIALS AND METHODS

All patients with histologically proven XGN were identified from the pathology database. Fourteen patients were diagnosed with XGN from January 2003 until December 2008. Eleven patients underwent preoperative CT and 13 studies (2 patients had two preoperative scans each) were available and retrieved from the digital image archive.

Access this article online

Quick Response Code:



Website:

www.clinicalimaging-science.org

DOI:

10.4103/2156-7514.84323

Copyright: © 2011 Rajesh A. This is an open-access article distributed under the terms of the Creative Commons Attribution License, which permits unrestricted use, distribution, and reproduction in any medium, provided the original author and source are credited.

This article may be cited as:

Rajesh A, Jakanani G, Mayer N, Mulcahy K. Computed Tomography Findings in Xanthogranulomatous Pyelonephritis. J Clin Imaging Sci 2011;1:45.

Available FREE in open access from: <http://www.clinicalimaging-science.org/text.asp?2011/1/1/45/84323>

Ten studies were performed on a 16-slice multidetector (MDCT) machine (Somatom Sensation 16, Siemens AG, Erlangen, Germany; tube voltage 120 kV, tube current 250 mA, section thickness 3 mm, and reconstruction interval of 1.5 mm). Two studies were performed on a single-slice helical machine (Philips Secura, Amsterdam, The Netherlands; tube voltage 130 kV, tube current 30 mA, 95 mA, section thickness 10 mm, reconstruction interval 8 mm, and pitch of 1.5). One study was on a 64-slice MDCT machine (Toshiba Aquilion, Tokyo, Japan; renal colic low dose protocol—tube voltage 120 kV, tube current 180 mA, section thickness 5 mm, and reconstruction interval 5 mm).

Nine of the 13 studies were contrast-enhanced studies. Nonionic contrast medium (1.5 ml/kg; 300 mg iodine/ml) was administered via a pump injector (Stellant, Medrad, Warrendale, Pennsylvania, USA) at a rate of 3 ml/sec with images obtained after a 60-sec delay in the portal venous phase of enhancement. Four patients underwent an unenhanced study for suspected renal stone disease.

The images were retrospectively reviewed on a workstation (AGFA Impax 5.1, Morstel, Belgium) by two consultant urologists (AR and KM). The kidneys were assessed for parenchymal inflammation and destruction, enlargement, calyceal dilatation, the presence of an obstructing renal calculus, demonstrable focal fat deposits, and any evidence of extrarenal extension. The renal size was estimated by measuring the maximum renal length on coronal images, and the anteroposterior diameter at the interpolar level of the renal hilum on the axial images. Extrarenal extension was defined as the presence of inflammatory changes in the perinephric tissues as evidenced by perinephric fat stranding, pararenal fascial thickening, the presence of related collections/abscesses or inflammation in the retroperitoneum, and adjacent abdominal organs.

RESULTS

Thirteen CT studies of 11 patients (6 females and 5 males) were analyzed. The mean age of the study population was 61.8 years (range 39–86 years). Ten patients had diffuse XGN changes on histology, while one patient had focal disease. All patients had unilateral disease. Renal enlargement was demonstrable on CT in all patients as an increase in either the AP dimension or renal length on the affected side [Table 1]. Nine patients (82%) had multiple dilated calyces and abnormal parenchyma. Six patients (55%) had a renal pelvis or upper ureter calculus causing obstruction. Three patients (27%) had focal fat deposits identifiable within

Table 1: Renal size (cm)

Patient	Affected Side	Renal length- Right	Renal length- Left	AP diameter - Right	AP diameter - Left
1	Right	16.1	9	11.8	6.5
2	Left	10	10.2	5	6.5
3	Left	10.7	12.5	6.4	9.7
4	Left	13	14.5	5.2	6.8
5	Right	13	11	7.3	4.6
6	Left	12.3	12.1	6.9	9.2
7	Left	10.9	13.6	5.6	8.8
8	Right	9.8	9.8	9.2	4.3
9	Left	9.8	13	6.2	10
10	Right	9.5	9.1	6	4.8
11	Right	13	9	6.5	5.3

the inflamed renal parenchyma. Two patients had renal abscesses. Ten patients (91%) had extrarenal extension of the inflammatory changes, with perinephric and pararenal space stranding and associated perirenal fascial thickening. Three patients (27%) demonstrated more extensive retroperitoneal inflammation, with abscesses within the ipsilateral psoas muscle and extension of inflammation to the abdominal wall. An associated splenic abscess was noted in a single case.

DISCUSSION

The etiology of XGN remains unclear, but patients are typically middle aged and diabetic female patients, who commonly present with recurrent urinary tract infections, flank pain, hematuria, and occasionally sepsis and weight loss.^[2-6] The main predisposing renal factor appears to be obstruction, and an obstructing renal calculus is present in up to 75% of cases. It is postulated that renal obstruction promotes recurrent renal tract infections that lead to an abnormal immune response that is responsible for the chronic changes and parenchymal destruction that ensues.^[7]

The nonspecific clinical presentation of patients with XGN was responsible for the difficult preoperative diagnosis of the condition, and as a result, a significant number of cases were diagnosed on histology after radical nephrectomy was performed for presumed renal cancer. An example of this difficulty in diagnosis before the advent of CT was highlighted in a retrospective analysis by Malek et al, in which the diagnosis of XGN was correctly made preoperatively in only 1 of 26 patients.^[8]

While clinical diagnosis is difficult, the pathological features of XGN are usually characteristic. Histologically, the inflammatory foci typically display a central nidus of active inflammation and debris surrounded by a granulomatous reaction in which foamy macrophages are prominent, the latter containing abundant cytoplasmic lipid that imparts a yellowish color grossly. These areas can be visualised

macroscopically as xanthomas^[1] [Figure 1].

When present, the CT equivalents of the typical pathology findings are quite characteristic, and as a result, CT has considerably improved the ability to diagnose XGN preoperatively. The typical CT findings are unilateral renal enlargement and parenchymal inflammation. Multiple areas of low attenuation are visualized within the kidney, representing dilated renal calyces and pus-filled cavities replacing destroyed renal parenchyma. On contrast-enhanced studies, the walls of the dilated calyces demonstrate enhancement due to the vascularity of the surrounding granulation tissue and compressed normal renal parenchyma^[9,10] [Figures 2 and 3].

Calyceal dilatation is commonly due to obstruction from a renal or upper ureteric calculus. In the present case series, an obstructing calculus was present in only six cases (55%)

[Figures 3 and 4]. Recent work by Loffroy et al demonstrated hydronephrosis in 90% of cases, with staghorn calculi present in 6 of 13 (46%) cases.^[11]

In the present series, unilateral renal inflammation and enlargement were the most consistent findings demonstrated on CT and were present in all patients. This suggests that comparative estimation of renal size should always be performed in the CT evaluation of every patient with suspected XGN. This can be accurately done on CT as supported by a recent study by Kang et al^[12] which compared the accuracy of various imaging modalities in estimating renal size. In their study, the authors conclude that the measurement of the renal length on coronal CT sections provides the most accurate estimation of renal size.^[12]

Extrarenal extension was characterized by stranding and inflammatory changes in the perinephric fat and associated

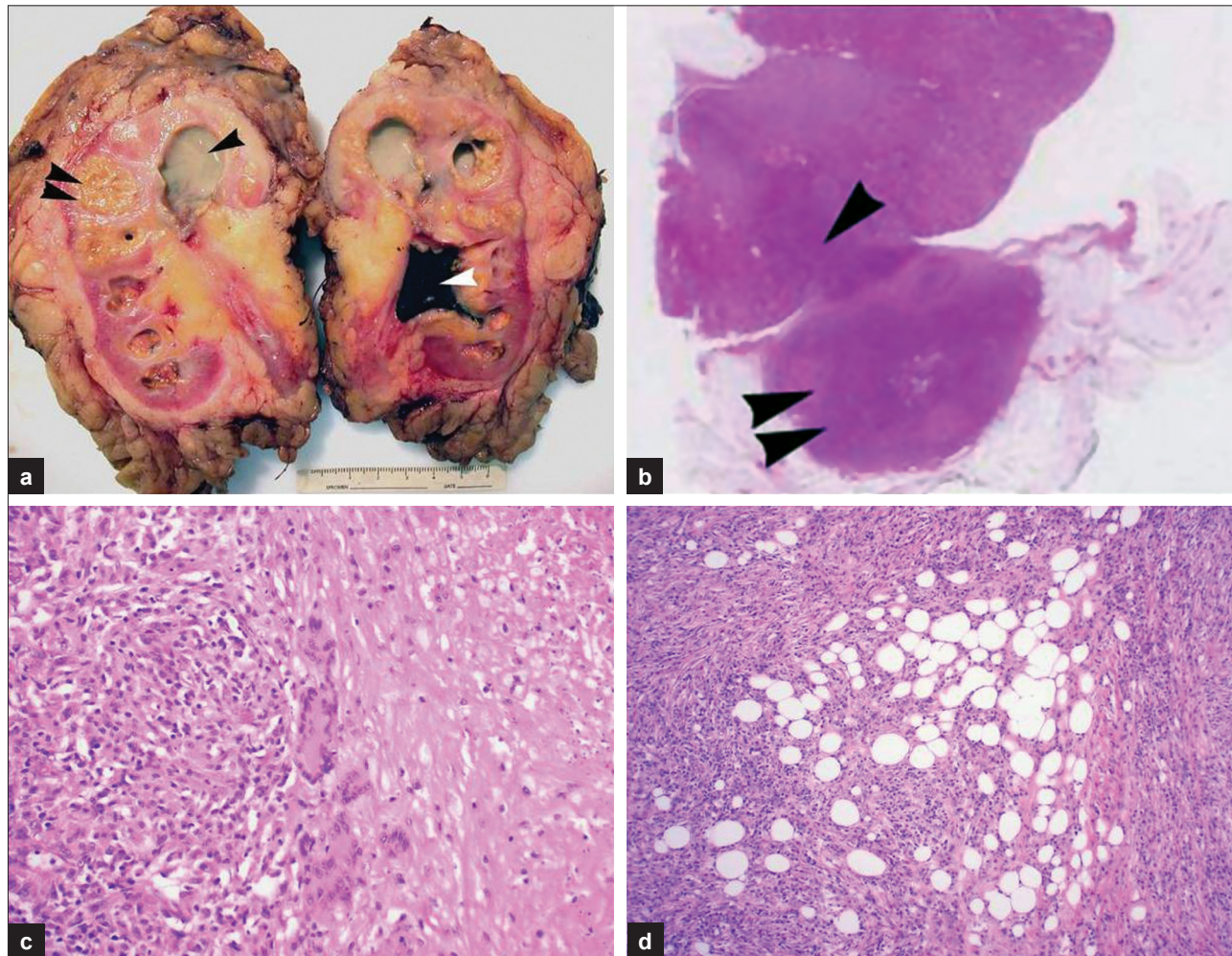


Figure 1: (a) Gross nephrectomy specimen showing characteristic lobulated xanthomatous lesions confined to the renal parenchyma (double arrowhead) caused by an obstructing “staghorn” calculus (white arrowhead) within the renal pelvis which has caused secondary hydronephrosis. The dilated upper pole calyces contain purulent green colored fluid (single black arrowhead). (b) H and E section showing focal XGN. Note the wedge-shaped area of cortical inflammation (arrowhead) in continuity with a larger nodular area extending into perinephric fat (double arrowhead). (c) Renal parenchymal granulomatous inflammation with multinucleate giant cells and focal necrosis (far right). The inflammatory infiltrate is rich in histiocytes, some of which have a foamy appearance reflecting high intracellular fat content. (d) The inflammatory reaction extends into perinephric fat (represented by the clear spaces) and with time will undergo organization and fibrosis.

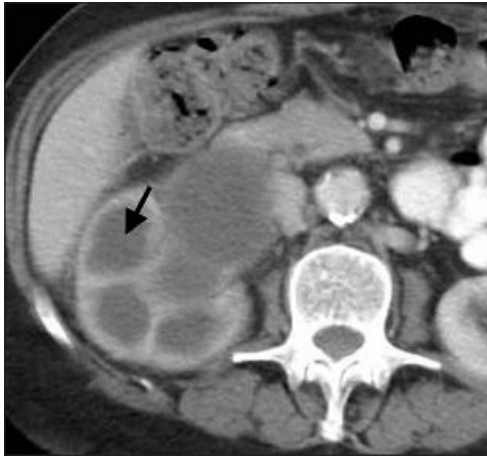


Figure 2: An 85-year-old female presented with weight loss and hypercalcemia. Contrast-enhanced CT shows multiple low attenuation areas (arrow) in right kidney surrounded by intensely enhancing walls. Low attenuation areas represent dilated calyces and pus-filled spaces replacing renal parenchyma.

thickening of the pararenal fascia [Figure 4]. A number of patients had more extensive extrarenal inflammation with abscess formation and variable involvement of the adjacent abdominal organs and retroperitoneum [Figure 5]. There are literature reports of extensive extra renal disease that extends posterolaterally to the abdominal wall. In these circumstances, patients may present with a draining cutaneous fistula.^[11,13] Abnormal fistulous communication with bowel has also been reported.^[14,15]

The pathologically distinguishing feature of xanthomas was infrequently observed, as only three patients (29%) had demonstrable focal fat deposits representing discrete xanthomas. Whether it is a useful distinguishing finding is debatable as there are other renal masses that may contain focal fat deposits within them, notably liposarcomas and

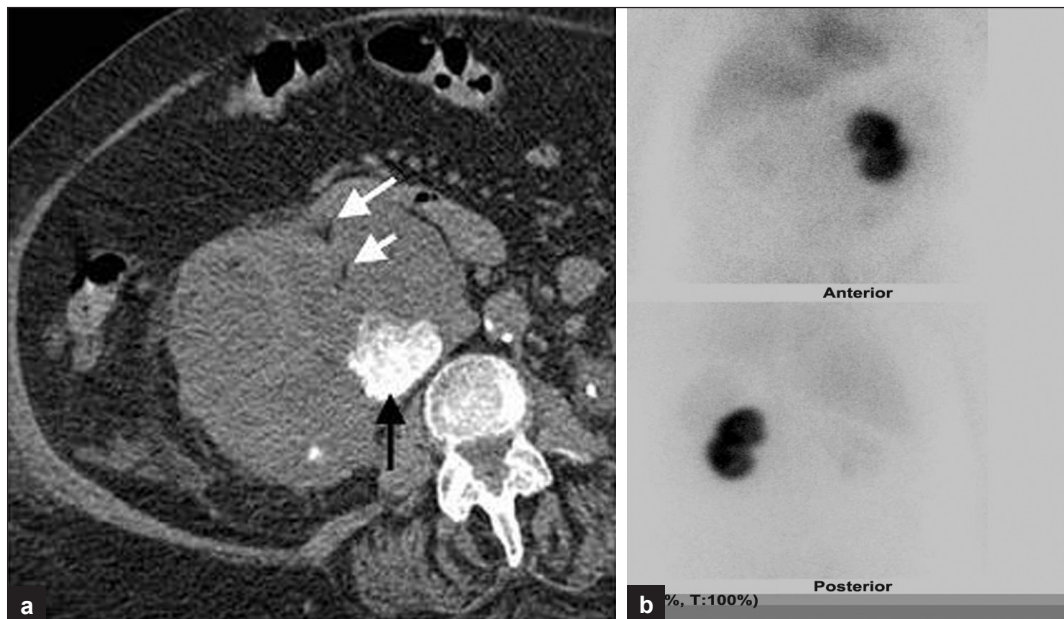


Figure 3: (a) XGN in an 82-year-old female with known renal stones who presented with obstructive uropathy and hyperkalemia. Noncontrast CT image shows right renal enlargement and dilated calyces with an obstructing renal calculus (black arrow). Also seen are focal xanthomas (white arrows). (b) DMSA image shows no uptake in right kidney and 100% function in left kidney. Histology post nephrectomy confirmed XGN.

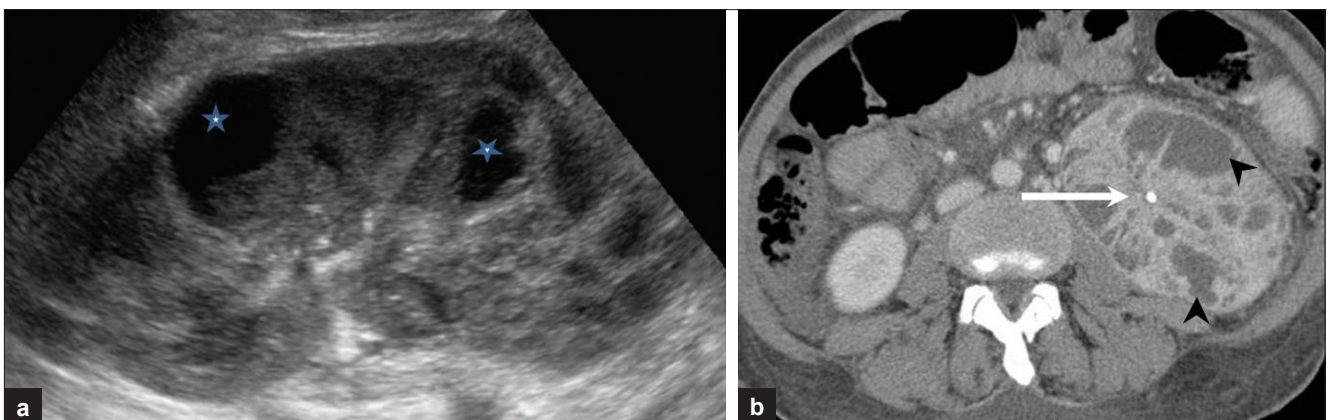


Figure 4: (a) XGN in a 40-year-old female with chronic pancreatitis, fever, and weight loss. Ultrasound image showed an enlarged kidney with focal cystic areas (stars), reported as likely renal abscesses. (b) Selected axial CT image shows multiple enhancing dilated calyces (black arrowheads) and an obstructing renal calculus (white arrow).

angiomyolipomas. To the best of our knowledge, there are no previous studies in the literature documenting the incidence of this finding. Table 2 is a summary of typical findings in XGN.

Focal XGN presents a particular diagnostic challenge as focal XGN changes may be misreported as renal cell carcinoma or lymphoma [Figure 6]. Focal XGN may be indistinguishable from other renal pseudotumors that include focal pyelonephritis and renal abscesses.^[16] In

Table 2: Summary of findings in XGN

Unilateral renal inflammation and enlargement
Dilated renal calyces
Obstructing renal or upper ureteric calculus
Extrarenal extension
Stranding and inflammatory changes in perinephric fat and thickening of the pararenal fascia
Abscess formation
Variable involvement of the adjacent abdominal organs and retroperitoneum



Figure 5: XGN in an 82-year-old male with perinephric inflammatory changes. There is perinephric stranding and thickening of the posterior pararenal fascia (white arrows). Also seen are focal xanthomas (black arrow).



Figure 6: Focal XGN in a 54-year-old with unexplained weight loss. Low attenuation lesion (23 HU) in lower pole of left kidney (black arrow) Note associated inflammation in the posterior perinephric space and thickened pararenal fascia (white arrows).

these cases, the diagnosis is almost inevitably made after nephrectomy. It is interesting to note that in the present series, perinephric stranding and pararenal fascial thickening were demonstrable in the single case of focal XGN. Conversely, one patient with histologically diffuse disease had no CT evidence of extrarenal extension. The evolving role of magnetic resonance imaging (MRI) in characterizing focal renal masses may prove useful in these cases, but MRI findings of XGN are nonspecific, and more work is needed to assess the diagnostic utility of this modality.

The limitations of this study were that it was a retrospective review of a small sample size. With increasing use of CT in the diagnosis of the condition, larger prospective series are expected to add to the existing literature in the coming years.

CONCLUSION

The most typical features of XGN on CT are unilateral renal enlargement and extrarenal extension of inflammatory changes. Their presence in a patient with constitutional symptoms and urinary tract infection should alert the radiologist to the possibility of this uncommon condition. Demonstrable focal fat deposits representing the pathologically distinguishing feature of xanthomas are an infrequent finding on CT.

REFERENCES

1. Kumar V, Abbas A, Fausto N, editors. Robbins and Cotran Pathologic Basis of Disease. 7th ed. Philadelphia, Pa: Saunders Elsevier; 2005.
2. Hayes WS, Hartman DS, Sesterbenn IA. Xanthogranulomatous pyelonephritis. *Radiographics* 1991;11:485-98.
3. Clapton WK, Boucaut HA, Dewan PA, Bourne AJ, Byard RW. Clinicopathological features of xanthogranulomatous pyelonephritis in infancy. *Pathology* 1993;25:110-3.
4. Fan CM, Whitman GJ, Chew FS. Xanthogranulomatous pyelonephritis. *AJR Am J Roentgenol* 1995;165:1008.
5. Dwivedi US, Goyal NK, Saxena V, Acharya RL, Trivedi S, Singh PB, et al. Xanthogranulomatous pyelonephritis: Our experience with review of published reports. *ANZ J Surg* 2006;76:1007-9.
6. Korke F, Favoretto RL, Bróglia M, Silva CA, Castro MG, Perez MD. Xanthogranulomatous pyelonephritis: Clinical experience with 41 cases. *Urology* 2008;71:178-80.
7. Craig WD, Wagner BJ, Travis MD. Pyelonephritis: radiologic-pathologic review. *Radiographics* 2008;28:255-277.
8. Malek RS, Elder JS. Xanthogranulomatous pyelonephritis: A critical analysis of 26 cases and of the literature. *J Urol* 1978;119:589-93.
9. Goldman SM, Hartman DS, Fishman EK, Finizio JP, Gatewood OM, Siegelman SS. CT of Xanthogranulomatous pyelonephritis: Radiologic-pathologic correlation. *AJR Am J Roentgenol* 1984;141:963-9.
10. Claes H, Vcneecken R, Oyen R, Van Damme B. Xanthogranulomatous pyelonephritis with emphasis on computerized tomography scan. *Urology* 1987;29:389-93.
11. Loffroy R, Guiu B, Watfa J, Michel F, Cercueil JP, Krausé D. Xanthogranulomatous pyelonephritis in adults: Clinical and

- radiological findings in diffuse and focal forms. *Clin Radiol* 2007;62:884-90.
12. Kang KY, Lee YJ, Park SC, Yang CW, Kim YS, Moon IS, et al. A comparative study of methods of estimating kidney length in kidney transplantation donors. *Nephrol Dial Transplant* 2007;22:2322-7.
 13. Devevey JM, Randrianantenaina A, Soubeyrand MS, Justrabo E, Michel F. Xanthogranulomatous pyelonephritis with nephrocutaneous fistula. *Prog Urol* 2003;13:285-9.
 14. Matsuoka Y, Arai G, Ishimaru H, Takagi K, Aida J, Okada Y. Xanthogranulomatous pyelonephritis with a renocolic fistula caused by a parapelvic cyst. *Int J Urol* 2006;13:433-5.
 15. Bianchi G, Franzolin N. Renojejunal fistula caused by xanthogranulomatous pyelonephritis. *Br J Urol* 1980;52:66.
 16. Bhatt S, MacLennan G, Dogra V. Renal pseudotumors. *AJR Am J Roentgenol* 2007;188:1380-7.

Source of Support: Nil, **Conflict of Interest:** None declared.